Escaping from the Shadow: Bottleneck-Aware UAV Placement for High-Throughput Relaying

Dongrak Choi*, Yongjae Yoo*, Yubin Choi*, Jeongyeup Paek†, Saewoong Bahk*
*Department of Electrical and Computer Engineering and INMC, Seoul National University, Seoul, Republic of Korea
†Department of Computer Science and Engineering, Chung-Ang University, Seoul, Republic of Korea
{drchoi, yjyoo, ybchoi24}@netlab.snu.ac.kr, jpaek@cau.ac.kr, sbahk@snu.ac.kr

***Abstract*—Cellular communication inevitably has shadow zones due to geographical and economical reasons. In shadow areas, using *unmanned aerial vehicle* (UAV) relay between the user and the base station can be a viable and immediate solution to enable high throughput communication instantly. However, the location and altitude of the UAV have a significant impact on end-to-end throughput, making relay placement critical. In this paper, we propose *UPS*, a UAV relay placement system that identifies the bottleneck between UE–UAV and UAV–BS links and continuously relocate the UAV to a position that meets the throughput criteria for high-quality live streaming. We measure real UE–UAV–BS links by flying a UAV in actual shadow zones, and evaluate in a trace-driven manner. Results show that *UPS* not only satisfies the highest requirement for up to ∼40% longer periods than compared schemes, but also achieves them faster.**

***Index Terms*—UAV, cellular communication, shadow zone, relay bottleneck, Wi-Fi**

I. Introduction

Shadow zones are where cellular connectivity is poor despite being (at a larger scale) within the coverage area of base stations. Even though cellular technology continues to evolve and improve, shadow zones exist due to geographical and economical reasons such as remote and rugged mountain terrains, urban canyons, and disaster-stricken zones. However, there are cases where high-throughput communication is required in such regions. An example is emergency rescue scenario on a mountain trail. Medical procedures performed by paramedics may need to be conducted under remote consultation with a physician, and high-quality video calls would be strongly preferred over simple voice [1]. Furthermore, IoT-based monitoring systems may demand intermittent high-rate communication in these zones. Installing more base stations is not only costly [2], but does not serve as an immediate solution. Thus, a more cost-effective method that instantly enables seamless communication in shadow zones is necessary.

Recently, significant advances have been made in *unmanned aerial vehicle (UAV)* technology, commonly referred to as drones [3]. The ease of control and deployment, mobility, and decrease in size and price have led to a significant interest in their potential applications in various domains [4]–[7]. In this context, we consider using UAVs as *relays* to provide temporary cellular communication in shadow zones for urgent missions [8]. A UAV serves as a bridge that enables line-of-sight (LoS) [9] communication between a ground user equipment (UE) [10] in a shadow zone and an adjacent base station (BS) [11].

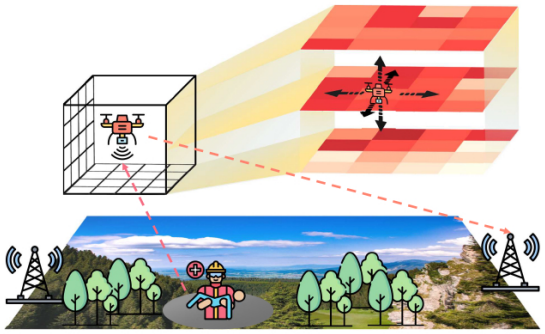

Fig. 1: Illustration of UAV relay in cellular shadow zone.

Cellular shadow zones indeed exist in the real-world [12]. We conduct experiments in actual shadow zones within an urban area with very good cellular (LTE and 5G) coverage to measure the throughput of ground UE-to-UAV Wi-Fi link and UAV-to-BS LTE link. Our measurements reveal that different altitudes and horizontal positions in 3-dimensional (3D) space above the shadow exhibit significantly different end-to-end throughput (§II), and the lower throughput of the two links act as a bottleneck. Then the key challenge is determining a good UAV position that achieves high overall network performance.

To address this challenge, we propose *UPS*, a *UAV placement scheme* that enables high throughput relay communication between a UE and a BS in shadow zones via a UAV (Fig. 1). *UPS* consists of four main components: *initial exploration*, *hovering determination*, *moving policy*, and *space pruning*. The four modules can detect the bottleneck between the UE–UAV and UAV–BS links, and quickly move the UAV in a direction expected to relieve the bottleneck to satisfy the throughput requirements of live video streaming.

We evaluate *UPS* through trace-driven analysis using a dataset of link measurements from real UAV flights at two

This work was supported by the MSIT (Ministry of Science and ICT) and IITP (Institute for Information & Communications Technology Planning & Evaluation), Korea, under the ITRC Support Program (IITP-2026-2021-0-02048) and Open RAN Education and Training Program (IITP-2026-RS-2024-00429088), and also partly supported by the National Research Foundation of Korea (NRF) grant funded by the Korea Government (MSIT) (No. RS-2024- 00359450).

979-8-3195-3248-0/26/$31.00 ©2026 IEEE

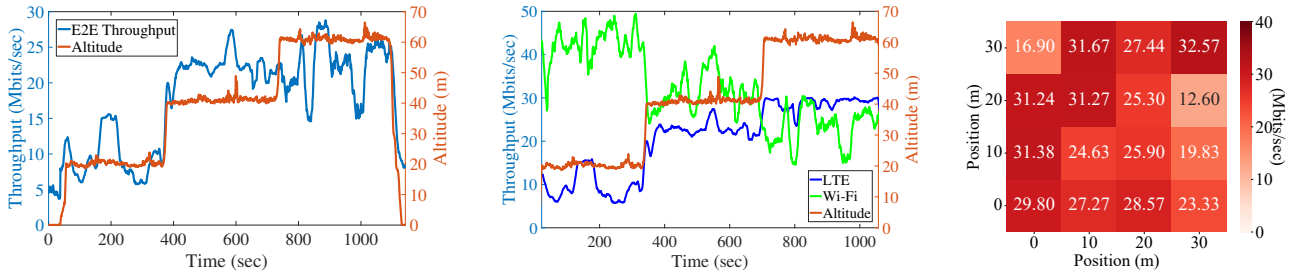

(a) E2E throughput **(b)** LTE and Wi-Fi throughput **(c)** E2E throughput at 40 m altitude

Fig. 2: Throughput at different altitudes during UAV flight.

different locations. The results show that *UPS* can find positions that satisfy the throughput requirements of live video streaming for up to ∼40% longer periods than other comparison schemes, with faster convergence.

The contributions of this work are as follows:

- Conduct real experiments in actual shadow zones to investigate the characteristics of UE–UAV–BS links in 3D space.
- Propose *UPS*, a bottleneck-aware relay placement scheme that continuously relocates the UAV to improve throughput.
- Evaluate *UPS* on real measurement data to show that it outperforms compared schemes in terms of throughput.

This paper is organized as follows: §II motivates our work, and §III presents prior work in the literature. We propose *UPS* in §IV and evaluate it in §V. §VI discusses limitations of our work, and §VII concludes the paper.

II. Motivational Study

We collect data from UE–UAV Wi-Fi link and UAV–BS LTE link during several UAV flight experiments in real shadow zones. We measure throughput, signal strength, and position information using smartphones mounted on the UAV with iPerf3 application and built-in GPS. Details about the experiment setup is described in §V-A.

In one experiment, the UAV takes off from a known 2D position and hovers for approximately 5 minutes at three different altitudes: 20 m, 40 m, and 60 m. Fig. 2a plots the end-to-end throughput between the ground user and connected base stations[1]. There is an improvement in throughput compared to the ground level as the UAV rises to 20 m above ground, yet remains low and unstable. At an altitude of 40 m, the UAV achieves notably higher throughput than 20 m while fluctuating significantly less than 60 m. To understand the varying trends in end-to-end throughput at different altitudes, Fig. 2b plots the throughput of the two individual links: UE–UAV Wi-Fi and UAV–BS LTE links. It shows that as the altitude increases, in general, the LTE throughput improves while that of Wi-Fi deteriorates. Furthermore, Fig. 2b matches Fig. 2a such that among the two links, the lower throughput link acts as the bottleneck to determine the end-to-end throughput.

[1]The iPerf3 measurements are against the backend server over the Internet. We verified that the wired bandwidth is sufficient and thus not the bottleneck.

In another experiment, the UAV hovers over each of the 4x4 horizontal grid points spaced 10 m apart at an altitude of 40 m for 5 minutes each. Fig. 2c presents the average throughput heatmap for each location, which reveals that the average end-to-end throughput varies significantly across 2D positions despite being only 10 m apart. The irregular trends may be due to non-line-of-sight (NLoS) conditions created by obstacles, multi-path fading, resource availability, and which base station is serving the UE. Such irregularities are more often observed in shadow zones.

We also investigate how throughput is related to the *received signal strength indicator* (RSSI) and *reference signal received power* (RSRP) for Wi-Fi and LTE, respectively (We omit figures due to page limit). For Wi-Fi, we observe relatively high correlation between RSSI and throughput. For LTE, the relationship between RSRP and throughput varies significantly depending on which base station the UE is connected to. This implies that predicting throughput from signal strength is infeasible, which is why we focus on throughput as a direct measure of performance for *UPS* design.

Lastly, we investigate how throughput could vary over time even at the same position. In Fig. 2a, while hovering for approximately 5 minutes at each altitude, the throughput remains relatively consistent at 40 m. In contrast, a significant variation was observed at 20 m, and throughput fluctuates noticeably at 60 m. These fluctuations are made at other locations as well. This means that the channel exhibits time-variant characteristics, and it is important to continuously re-evaluate positions for higher throughput.

Through aforementioned experiments, we found that the placement of UAV relay has a significant impact on end-to-end throughput, and either the UE–UAV Wi-Fi or UAV–BS LTE link acts as the bottleneck. There is a general trend in throughput with altitude (Fig. 2b), but relatively more irregularities in the horizontal 2D plane (Fig. 2c), and they could change over time. Then, searching for UAV positions that enhance the end-to-end throughput of a ground user becomes the key challenge, and an intelligent placement scheme for the relay UAV is needed, which motivates our work.

III. Related Work

Recent studies on UAV relays have focused on maximizing end-to-end throughput [13], minimizing outage probability [14], expanding coverage [15], and addressing eavesdropping threats [16], [17]. Foremost, optimal placement of UAV is critical in maximizing throughput within a relay system. For example, Shams ur Rahman *et al.* [18] proposed a scheme where user positions and data rate requirements are sent to a centralized SDN controller to compute the optimal positions for maximizing throughput. Ding Ma *et al.* [19] aims to maximize throughput by optimizing the height of the UAV using a particle swarm optimization algorithm to address non-deterministic polynomial problem.

Aforementioned works have all taken theoretical and/or simulation-based approaches. Only a few studies have used real data from actual UAV flight experiments. Kai Li *et al.* [20] developed a secure multi-hop aerial relay system named BloothAir based on BLE, and utilized two actual UAVs for evaluation. Homayouni *et al.* [21] presented field trials to understand the throughput performance of UAVs across various LTE bands and altitudes. Yoo *et al.* [22] proposed an altitude selection algorithm for high-quality cellular connectivity on UAVs based on real measurements. Omid Esrafilian *et al.* [23] conducted real experiments to explore UAV acting as a relay to enhance connectivity within a Wi-Fi based wireless mesh network on the ground.

However, few works have measured both the LTE and Wi-Fi links in both directions on an actual UAV relay to assess the overall performance. Rajeev Gangula *et al.* [24] configured two LTE link relays using OpenAirInterface (OAI) to enable an automatic placement algorithm identifying the location with maximum channel gain. Yet, it only considers signal strength, showing simple altitude analysis. Moreover, existing works do not demonstrate throughput sufficient for video streaming.

IV. *UPS* Design

This section presents the design of the proposed bottleneck-aware UAV placement scheme for communication relaying.

A. Objective and System Model

The goal of *UPS* is to quickly place the UAV to satisfy the high throughput requirement of video streaming in shadow zones for urgent missions. The UAV establishes a connection with the ground user equipment (UE) in the shadow zone through Wi-Fi, and with nearby base stations via cellular (LTE). The UAV measures its own throughput and is aware of which link, either the UE–UAV or UAV–BS link, is the bottleneck of end-to-end throughput. The mission area is discretized into grid points, and the UAV can select its movement in 7 distinct directions: *up, down, left, right, forward, backward, and hover*. As UAV arrives at a new position, it will hover for T_q seconds to observe the throughput of each link, and move to another point to alleviate the bottleneck if necessary. The UAV continues to hover at current position when the throughput requirements are fully satisfied. Given this scenario, we design *UPS* consisting of four modules: *initial exploration*, *hovering determination*, *moving policy*, and *space pruning*. The parameters for system design are detailed in Table I.

TABLE I: Notation and parameter table.

Notation	Definition
$P(x, y, z)$	Position of UAV
T_q	Observation period / Length of queue (e.g. 15 sec)
T_s	Sampling period (5 sec in our implementation)
$Thrp_w$	UE–UAV Wi-Fi throughput for T_q
$Thrp_c$	UAV–BS LTE throughput for T_q
$Thrp_{e2e}$	End-to-end throughput for T_q
S_o	Observation state
N	Number of hovering states (3 in our implementation)
S_n	Hovering state ($1 \leq n \leq 3$)
Th_n	Throughput threshold ($1 \leq n \leq 3$)
c_n	Counter for transition ($1 \leq n \leq 3$)
d_{max}	UAV maximum travel distance from UE

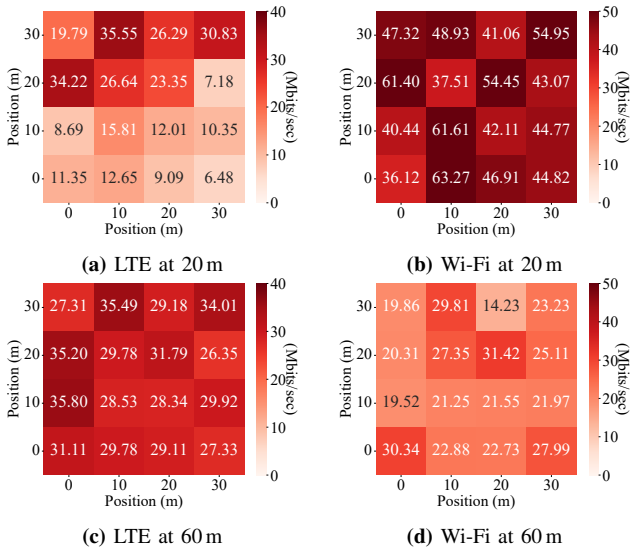

(a) LTE at 20 m **(b)** Wi-Fi at 20 m

(c) LTE at 60 m **(d)** Wi-Fi at 60 m

Fig. 3: LTE and Wi-Fi throughput at different altitudes. Note the variation even at 10 m distances, vertically and horizontally. (Other altitudes omitted for brevity due to page limit)

B. Initial Exploration

This module attempts to quickly find a mission starting point right after takeoff by exploiting throughput tendency. For example, Fig. 3 presents the average measured Wi-Fi and LTE throughputs through heatmap images at each of 4x4 grid points at each altitude. The positions with high LTE throughput are clustered together at 20 m altitude, and as altitude increases further, other points with high throughput are located around this cluster. Otherwise, areas with low throughput are often surrounded by other low-throughput positions. On the other hand, Wi-Fi throughput shows the inverse relationship with distance between the UAV and UE

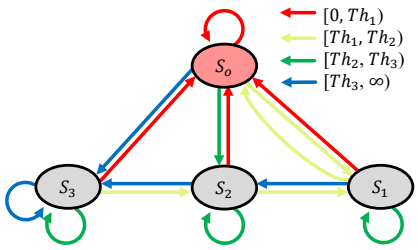

Fig. 4: State diagram of hovering determination module.

Threshold	Resolution	Frame Rate	Recommended Bitrate
Th_3	4K / 2160p	60fps	35 Mbits/sec
Th_2	4K / 2160p	30fps	30 Mbits/sec
Th_1	2K / 1440p	60fps	24 Mbits/sec

TABLE II: Throughput threshold and recommended bitrate setting (Mbps) H.264 for Youtube live streaming [25].

(UE is positioned at (20, 10, 0)), consistent with the nature of Wi-Fi signal attenuation.

Based on the observed trends, *UPS* finds a mission starting point by predicting regions likely to exhibit higher data rates. This approach can be implemented by visiting the initial exploration points where the UAV will measure end-to-end throughput right after takeoff. For example, we set the initial exploration points as the innermost points at the lowest altitude, which follows the path P(20, 10, 20), P(20, 20, 20), P(10, 20, 20), and P(10, 10, 20) in Fig. 3. The UAV will hover at such points for T_q, and initiate the mission from the position recording the highest average throughput among them. This approach allows for faster convergence to optimal hovering points by exploring places where good throughput is expected.

C. Hovering Determination

The UAV hovers at positions that satisfy the throughput requirement. However, a grid point satisfying the requirement may not continue to do so as time passes due to the time-variant channel (§II). Thus the UAV must determine whether it should continue to hover at its current position or move not to miss out on opportunities that may offer higher throughput. To address this challenge, we propose a hovering determination algorithm illustrated by a state diagram in Fig. 4. The three *hovering states* S_1, S_2, and S_3 are determined by the three throughput requirement thresholds Th_1, Th_2, and Th_3 based on the live streaming service Table II. T_q and T_s are set to 15 seconds and 5 seconds each.

The *hovering determination* operates as follows. In S_o state, the UAV moves to an adjacent point to seek better points by choosing one possible direction except *hover*, and then observes the throughput for T_q. Given the clear hierarchy of throughput thresholds, it can determine which level the measured average throughput falls into. As shown in Fig. 4, if end-to-end throughput satisfies any of the thresholds, the UAV begins to stay at current point by transiting to the corresponding hovering state, believing it satisfies the requirement at its location. If none of the three levels are met, S_o is repeated until it finds points with any of the thresholds.

Algorithm 1 MOVING POLICY

Input: $Thrp_{e2e}$, $Thrp_w$ and $Thrp_c$
Output: $P(x, y, z)$
Procedure:
if $mean(Thrp_{e2e}) \geq Th_1$ **then**
  Follow *Hovering Determination* ▷ Fig. 4
end if
if $mean(Thrp_{e2e}) < Th_1$ **or** $c_1 \geq ceil(T_q/T_s)$ at S_1 **then**
  if $mean(Thrp_c) < mean(Thrp_w)$ **then**
    Move to improve LTE (further from UE)
  end if
  if $mean(Thrp_c) \geq mean(Thrp_w)$ **then**
    Update d_{max} for *Space Pruning* ▷ §IV-E
    Move to improve Wi-Fi (toward UE)
  end if
end if

The *hovering counters* control the transition between hovering states. While in a hovering state, the UAV receives updates on the level of throughput requirement at each T_s. There are c_1, c_2 and c_3 counters, and if the average throughput for T_s satisfies Th_n, then c_n increments by 1. The transition to a lower or upper hovering state only occurs when c_1 or c_3 consecutively increases to $ceil(T_q/T_s)$ each. The counters will reset if they stop increasing or the hovering state changes. If any counter does not increase for T_q, the UAV will transit to the S_o and moves to a new grid point.

Thus, even if initially settled in the highest state, the UAV may move to another position for better throughput if the channel conditions worsen. In contrast, the UAV assigned to a lower hovering state will take more opportunities to hover if the throughput improves at that location. In this way, the UAV continuously searches for positions that can yield even higher throughput.

D. Moving Policy

This policy controls the movement of the UAV in a way that alleviate the bottleneck link to enhance end-to-end throughput based on its awareness of where the bottleneck lies. Alg. 1 is the pseudocode of the policy. The UAV continuously measures the UE–UAV and UAV–BS links from its current grid point and calculates the average throughput of each link. By comparing these averages, the UAV determines which link is the bottleneck and then shifts the grid point in a direction that improves the throughput; At a high-level, the UAV flies towards the ground user to improve the Wi-Fi link, whereas it selects a points that is further away from UE to improve the cellular link. By leveraging this policy, *UPS* improves the bottleneck link and increases the end-to-end throughput.

E. Space Pruning

This module aims to reduce the mission area to decrease the time needed in finding optimal positions. For this purpose, *UPS* sets the maximum distance d_{max} that the UAV can travel by focusing on UE–UAV Wi-Fi link. Specifically, if the UE–UAV Wi-Fi link operates as the bottleneck link, it is obvious that the end-to-end throughput will deteriorate by moving

(a) Aquilar 1 & M16 **(b)** Aquilar 2 & MK-15 **(c)** AD7200 + laptop

Fig. 5: Equipment used for the experiments.

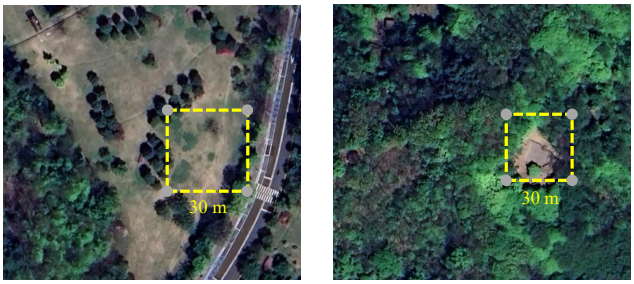

(a) Place 1 **(b)** Place 2

Fig. 6: Two experiment sites: real LTE shadow zones.

further away from the ground UE due to signal attenuation (Fig. 3). Therefore, the UAV need not visit the grid points further from the UE. In such situation, *Space Pruning* sets d_{max} as the distance between the current position of the UAV and the UE in Alg. 1 Line 9, ensuring that the UAV does not exceed this distance. d_{max} is updated if the same situation occurs at a shorter distance, or if the UE moves. Pruning the mission area in such a manner reduces the exploration distance, enabling the UAV to converge more swiftly.

V. Evaluation

We evaluate *UPS* by emulating a UAV relay system based on the real-world data measured at two experimental sites[2], and comparing it against four different alternative schemes.

A. Experiment Setup

The hardware and software configurations for our real-world outdoor experiments are as follows.

UAV: We use Argosdyne Aquilar (Fig. 5a & Fig. 5b) models which are connected to Android-based controllers. They provide automatic flight mode along a pre-defined route setting based on GPS coordinates. We register the coordinates of grid points in the 3D airspace at each site, then specify these points in the controller for UAV flight. Two smartphones, Galaxy S22 and S22+, are mounted on the UAVs for measuring LTE and Wi-Fi links, respectively. The speed of UAV is set to 5 m/sec.

Ground User Equipment: establishes a link with the UAV via IEEE 802.11ac Wi-Fi using TP-Link Talon AD7200 AP with 20MHz bandwidth, and connect a laptop through a serial port to act as a UE (Fig. 5c).

[2]We use emulation because our UAVs do not provide capability for real-time software-controlled maneuver which is required by *UPS*.

Server: Data sent by the ground user via UAV ultimately reaches the backend server which measures the throughput using iPerf3 on Linux. We verified that the network bandwidth between the base stations and the server is sufficient such that it does not act as the bottleneck of the relay system.

Measurement Applications: We use iPerf3 on the AP (connected to a laptop), smartphones, and server to record throughput at 1-sec intervals. We also developed a custom Android application to collect GPS, altitude, and signal strength data on the smartphones mounted on the UAV.

Experiment Sites: We conduct experiments at two different actual *shadow zones* where *cellular connectivity is unavailable on the ground but accessible higher up in the air*. 'Place 1' is a park within a university campus, and 'Place 2' is a hiking trail on a mountain completely enclosed within a large city. Place 1 (Fig. 6a) is configured as $4 \times 4 \times 3$ grid points where each grid point is spaced 10 m apart in the 2-D plane with three different altitudes: {20, 40, 60} m. Place 2 (Fig. 6b) has $4 \times 4 \times 4$ grid points with altitudes: {30, 40, 50, 60} m.

Comparison Schemes: Since there is no similar prior work with real implementation, we design several alternative schemes to compare the performance of *UPS*:

- **Oracle** jumps to any point with the highest throughput every second, assuming it knows the achievable throughput at all other points. *Note that this is ideal and unattainable.*
- **Prophet** assumes knowledge of throughput at adjacent points within one step away from the current position (without observation), and moves to the point with the highest throughput. *This is also unrealistic in a real system.*
- **Naive** observes the throughput at its current location for T_s and moves in a direction that improves the bottleneck among UE–UAV or UAV–BS links when it fails to meet the target throughput. Three variations will be compared according to each requirement: *Naive24*, *30*, and *35*.
- **Random** chooses the next grid point randomly from the seven possible/adjacent points, then stays for T_s before the next movement.

The values in Table I are set empirically for the experiments as T_q= 15 seconds, T_s= 5 seconds, and N=3. The three levels of throughput requirements are determined by referencing Youtube live streaming criteria in Table II.

B. End-to-End Throughput

The goal is for our UAV to move to positions that can achieve the throughput requirement of live video streaming to the extent possible. Fig. 7 plots the end-to-end throughput of each scheme at the two experiment sites. At Place 1 (Fig. 7a), *UPS* demonstrates higher throughput than all other schemes except for the Oracle, achieving performance levels sufficient to transmit 4K 60fps. *Prophet* does reach the throughput of *UPS*, but at a significantly later time. Even with the knowledge of achievable throughput one grid-point away, it is insufficient to quickly locate the UAV to satisfy the highest criteria. While *Naive* does improve its throughput, it remains at a lower level than *UPS*. As expected, *Random* performs the worst due to lack of any informed decisions.

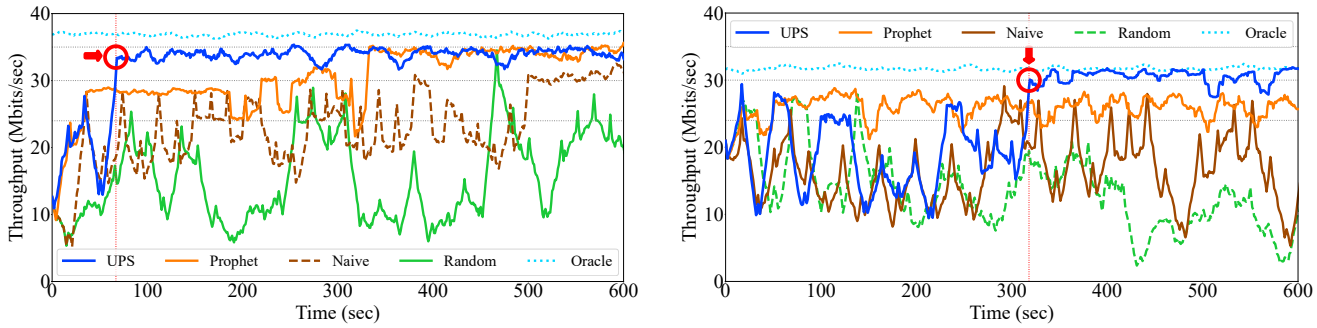

(a) Place 1 **(b)** Place 2

Fig. 7: End-to-end throughput comparison.

A similar pattern can be observed at Place 2 as well (Fig. 7b). Unlike Place 1, however, there are no grid points satisfying 35 Mbps at Place 2, inevitably settling for grid points with throughput over 30 Mbps. *Prophet* manages to maintain a relatively constant throughput, but fails to locate areas with more than 30 Mbps. This suggests that, due to the movement characteristics of *Prophet*, it settled into a local optimum with higher throughput than the surrounding areas without finding the globally highest throughput point. In contrast, the *UPS* eventually finds the grid points that provide high uplink throughput similar to those used by the *Oracle* after about 320 seconds. Based on the results, it can be concluded that *UPS* effectively places UAV to grid points that can satisfy the throughput requirements.

C. Satisfaction Duration Ratio

Table III presents the proportion of time each scheme satisfies the stepwise uplink live streaming criteria in Table II relative to the total mission time. At Place 1, there exist a location that satisfies the highest requirement criteria at any given time, as indicated by the result of *Oracle*. *UPS* shows the highest satisfaction rate for the three criteria compared to other schemes excluding *Oracle*. Specifically, *UPS* secures 41.83% more time capable of transmitting 4K 60fps compared to other schemes. This is lower than 94.50% of *Oracle*; however *Oracle* is unattainable in reality.

At Place 2, however, the time and grid points serving the highest standard of 35 Mbps constitute only 1% of all measurement samples. Therefore, achieving over 30 Mbps becomes important. Accordingly, *UPS* satisfies the 4K 30fps standard more often than any other scheme (except for the *Oracle* of course). In particular, *Prophet* records 23.17% lower satisfaction ratio than *UPS* due to it falling into a local optimum. For the lower criterion of 2K video, *UPS* shows lower satisfaction ratio compared to *Prophet* and *Naive24* because it continues to move for a location with better throughput without settling for 2K; Again, note that *Prophet* assumes knowledge of future, and *Naive24* settles for 2K without searching further. In conclusion, *UPS* is able to meet the higher throughput requirement of high quality live video streaming for longer periods than other schemes.

Location	Place 1 (%)			Place 2 (%)		
Resolution	4K	4K	2K	4K	4K	2K
Frame Rate	60fps	30fps	60fps	60fps	30fps	60fps
UPS	**41.83**	80.50	90.83	0.00	**42.50**	60.00
Prophet	23.17	52.17	91.33	0.00	19.33	78.33
Naive35	1.83	19.33	49.33	0.00	1.67	24.50
Naive30	1.33	18.00	64.83	0.00	4.50	25.33
Naive24	5.83	24.50	68.67	0.00	19.50	75.67
Random	2.00	6.50	19.67	0.00	3.33	14.67
Oracle	94.50	100.0	100.0	1.00	97.83	100.0

TABLE III: Throughput requirement of satisfied time ratio.

VI. Limitations and Future Work

Our system model quantized the mission area into discrete grid points. In reality, however, the positions of the UAVs will be continuous, and this approach excludes the possibility that the positions not investigated between grid points could offer better end-to-end throughput.

We plan to consider a wider range of variables to enhance end-to-end throughput more efficiently. For example, if the direction in which the signal strength increases is known before the UAV moves, possibly by utilizing the directionality of an antenna, this information could assist in determining the next movement direction. In addition, since there may be multiple base stations nearby, knowing the status of the currently supported base station could enable the UAV to move closer to another base station where higher throughput is expected.

VII. Conclusion

Through real flight experiments in actual shadow zones, we identified throughput trends and bottlenecks between UE–UAV Wi-Fi link and UAV–BS LTE link in 3D airspace. Based on those observations, we proposed *UPS*, a UAV placement scheme that enables high throughput communication relaying to ground users in cellular shadow areas. Evaluation results show that *UPS* satisfies the end-to-end throughput requirements of high-quality live video streaming for longer periods with faster convergence than other comparable schemes.

REFERENCES

[1] H. Ecker, S. Wingen, S. Hamacher, F. Lindacher, B. W. Böttiger, and W. A. Wetsch, "Evaluation Of CPR Quality Via Smartphone With A Video Livestream – A Study In A Metropolitan Area," *Prehospital Emergency Care*, vol. 25, no. 1, pp. 76–81, 2021.

[2] E. Kalantari, H. Yanikomeroglu, and A. Yongacoglu, "On the Number and 3D Placement of Drone Base Stations in Wireless Cellular Networks," in *IEEE 84th Vehicular Technology Conference (VTC-Fall)*, 2016.

[3] G. Geraci, A. Garcia-Rodriguez, M. M. Azari, A. Lozano, M. Mezzavilla, S. Chatzinotas, Y. Chen, S. Rangan, and M. D. Renzo, "What Will the Future of UAV Cellular Communications Be? A Flight From 5G to 6G," *IEEE Communications Surveys & Tutorials*, vol. 24, no. 3, pp. 1304–1335, 2022.

[4] N. Zhao, W. Lu, M. Sheng, Y. Chen, J. Tang, F. R. Yu, and K.-K. Wong, "UAV-Assisted Emergency Networks in Disasters," *IEEE Wireless Communications*, vol. 26, no. 1, pp. 45–51, 2019.

[5] W. Shi, J. Li, N. Cheng, F. Lyu, S. Zhang, H. Zhou, and X. Shen, "Multi-Drone 3-D Trajectory Planning and Scheduling in Drone-Assisted Radio Access Networks," *IEEE Transactions on Vehicular Technology*, vol. 68, no. 8, pp. 8145–8158, 2019.

[6] D. Orfanus, E. P. de Freitas, and F. Eliassen, "Self-Organization as a Supporting Paradigm for Military UAV Relay Networks," *IEEE Communications Letters*, vol. 20, no. 4, pp. 804–807, 2016.

[7] D. Ryoo, Y. Yoo, J. Paek, and S. Bahk, "NOVA: Navigation Optimization via UWB-Assisted Iterative Path Planning for UAV Delivery," in *Proceedings of The IEEE International Conference on Computer Communications (INFOCOM)*. IEEE, May 2026.

[8] H. Asano, H. Okada, C. B. Naila, and M. Katayama, "Flight Model Using Voronoi Tessellation for a Delay-Tolerant Wireless Relay Network Using Drones," *IEEE Access*, vol. 9, pp. 13 064–13 075, 2021.

[9] J. Park, H. Kim, and S. Bahk, "LoS/NLoS Detection based Authentication for IoT Systems," in *IEEE Global Communications Conference (GLOBECOM)*, 2020, pp. 1–6.

[10] H. Tanaka, N. Matsui, Y. Watanabe, H. Okada, and M. Katayama, "Experimental Evaluation of a Wireless LAN Relay System Using Unmanned Aerial Vehicles," in *Proc. IEEE Vehicular Technology Conference*, 2021, pp. 1–6.

[11] M. Alzenad, A. El-Keyi, F. Lagum, and H. Yanikomeroglu, "3-D Placement of an Unmanned Aerial Vehicle Base Station (UAV-BS) for Energy-Efficient Maximal Coverage," *IEEE Wireless Communications Letters*, vol. 6, no. 4, pp. 434–437, 2017.

[12] J. Sang, Y. Yuan, W. Tang, Y. Li, X. Li, S. Jin, Q. Cheng, and T. J. Cui, "Coverage Enhancement by Deploying RIS in 5G Commercial Mobile Networks: Field Trials," *IEEE Wireless Communications*, vol. 31, no. 1, pp. 172–180, 2024.

[13] Y. Zeng, R. Zhang, and T. J. Lim, "Throughput Maximization for UAV-Enabled Mobile Relaying Systems," *IEEE Transactions on Communications*, vol. 64, no. 12, pp. 4983–4996, 2016.

[14] S. Zhang, H. Zhang, Q. He, K. Bian, and L. Song, "Joint Trajectory and Power Optimization for UAV Relay Networks," *IEEE Communications Letter*, vol. 22, no. 1, pp. 161–164, 2018.

[15] E. Arribas, V. Mancuso, and V. Cholvi, "Coverage Optimization with a Dynamic Network of Drone Relays," *IEEE Trans. Mobile Comput.*, vol. 19, no. 10, pp. 2278–2298, 2020.

[16] Y. Ning and R. Chen, "Secure UAV Relay Communication via Power Allocation and Trajectory Planning," *IEEE Systems Journal*, vol. 16, no. 4, pp. 6243–6252, 2022.

[17] Z. Wang, J. Guo, Z. Chen, L. Yu, Y. Wang, and H. Rao, "Robust secure UAV relay-assisted cognitive communications with resource allocation and cooperative jamming," *Journal of Communications and Networks*, vol. 24, no. 2, pp. 139–153, 2022.

[18] S. ur Rahman, G.-H. Kim, Y.-Z. Cho, and A. Khan, "Positioning of UAVs for throughput maximization in software-defined disaster area UAV communication networks," *Journal of Communications and Networks*, vol. 20, no. 5, pp. 452–463, 2018.

[19] D. Ma, Z. Feng, and Y. Qin, "Optimization of Throughput Maximization of UAV as Mobile Relay Communication System," in *International Conference on Virtual Reality and Intelligent Systems (ICVRIS)*, 2020, pp. 798–801.

[20] K. Li, N. Lu, J. Zheng, P. Zhang, W. Ni, and E. Tovar, "BloothAir: A Secure Aerial Relay System Using Bluetooth Connected Autonomous Drones," *ACM Transactions on Cyber-Physical Systems*, vol. 5, no. 3, April 2021.

[21] S. Homayouni, M. Paier, C. Benischek, G. Pernjak, M. Leinwather, M. Reichelt, and C. Fuchsjäger, "On the Effect of Cellular-Connected Drones on Terrestrial Users: Field Trials," in *13th International Congress on Ultra Modern Telecommunications and Control Systems and Workshops (ICUMT)*, 2021, pp. 27–31.

[22] Y. Yoo, J. Suh, D. Choi, J. Paek, and S. Bahk, "ASCEND: Altitude Selection for High-quality Cellular Connectivity on Drones," *IEEE Transactions on Vehicular Technology*, vol. 75, no. 1, pp. 211–222, January 2026.

[23] O. Esrafilian, R. Gangula, and D. Gesbert, "Autonomous UAV-aided Mesh Wireless Networks," in *IEEE Conference on Computer Communications Workshops (INFOCOM WKSHPS)*, 2020, pp. 634–640.

[24] R. Gangula, O. Esrafilian, D. Gesbert, C. Roux, F. Kaltenberger, and R. Knopp, "Flying Rebots: First Results on an Autonomous UAV-Based LTE Relay Using Open Airinterface," in *IEEE International Workshop on Signal Processing Advances in Wireless Communications (SPAWC)*, 2018, pp. 1–5.

[25] Google Youtube, "Youtube Live Encoder Settings, Bitrates, and Resolutions," 2024. [Online]. Available: https://support.google.com/youtube/answer/2853702